Kinematic and Dynamic Approaches in Gait Optimization for Humanoid Robot Locomotion

Ramil Khusainov[1], Alexandr Klimchik[1(✉)], and Evgeni Magid[2]

[1] Intelligent Robotic Systems Laboratory, Innopolis University, Innopolis City, Russian Federation
r.khusainov@innopolis.ru, a.klimchik@innopolis.ru

[2] Higher Institute of Information Technology & Information Systems, Kazan Federal University, Kazan, Russian Federation
magid@it.kfu.ru

Abstract. Humanoid robot related research keeps attracting many researchers nowadays because of a high potential of bipedal locomotion. While many researchers concentrate on a robot body movement due to its direct contribution to the robot dynamics, the optimality of a leg trajectory has not been studied in details yet. Our paper is targeted to decrease this obvious gap and deals with optimal trajectory planning for bipedal humanoid robot walking. The main attention is paid to maximization of locomotion speed while considering velocity, acceleration and power limitations of each joint. The kinematic and dynamic approaches are used to obtain a desired optimal trajectory. Obtained results provide higher robot performance comparing to commonly used trajectories for control bipedal robots.

Keywords: Humanoids · Bipedal walking · Optimal trajectory planning

1 Introduction

Nowadays one of the most challenging tasks in robotics is developing multipurpose terrain robot which could perform various tasks, including operations in difficult and dangerous conditions. Such operations may require humanlike skills to overcome obstacles and get through environment, which was originally designed for a human. That is why it is critically important to develop humanoid robots, which are similar to human body in their size, weight and locomotion characteristics. Many theoretical and experimental researches have been done in the field of biped robots during three past decades and many notable developments have been achieved [1]. There are various practically realized systems, from the simplest cases of planar robots, to the most advanced robots, with many Degrees of Freedom (DoF) [2–4].

However, we are still very far from widespread use of humanoids. Mainly this is because biped robots' poor locomotion abilities and its ability to fall

K. Madani et al. (eds.), *Informatics in Control, Automation and Robotics*,
Lecture Notes in Electrical Engineering 430, https://doi.org/10.1007/978-3-319-55011-4_15

down. Although there are some efficient algorithms for the several application areas of humanoid robots [5], but it is very difficult to merge all of them into one efficient system because the overall system's complexity becomes extremely high. Especially the problem manifests itself when robot moves on rough terrain, steep stairs, and in environments with obstacles. Hence, robot stability related research keeps attracting many researchers nowadays in order to propose good robot locomotion control algorithms and to prevent a biped robot from falling down.

Walking stability can be divided into static and dynamic. The static stability can be verified through being the center of gravity (COG) in the stability area (supporting polygon). There are several stability criteria for biped walking but mostly the dynamic stability is verified via Zero Moment Point (ZMP) criterion [6]. ZMP is a point on the ground at which the total moments due to ground reaction force becomes zero. In other words, the influence of all ground forces can be replaced by one force applied in ZMP point. In order to achieve a dynamically stable gait the ZMP should be within the support polygon, at every time instance. The assumption of ZMP approach is that dynamic biped walking can be decomposed into two parts, a walking pattern generation and a stabilization around it. In this paper we discuss the first part. The research studies on walking gate generation can be classified into three main groups, i.e. robot modeling, walking pattern generation and gait parameter optimization.

Robot modeling works on reducing complexity of robot motion dynamics with certain approximation error. Here compromise is required between model error and computational cost. In many research studies inverted pendulum model (IPM) utilized, which approximates robot as a single point mass concentrated at the center of mass (COM) [7]. The model is simple but leads to significant ZMP error since usually legs of the robot are heavy and cannot be neglected. An alternative here is utilization multiple masses IPM (MMIPM) model robot [8], which consists multiple point masses. To make model effective it is required to choose proper number of point masses to ensure optimality from cost/error point of view. Sato et al. [9] proposed three mass IPM (3MIPM) with point masses at COM and feet, Ha and Choi [10] proposed virtual height IPM (VHIPM) that has dynamics form of IPM for multiple mass model. In practice, model choice highly depends on the gait generation and control methods. There are two main approaches to generate walking pattern: using online or/and offline methods. In online methods, computational cost is the main issue and full body dynamics cannot be processed. Therefore, simplified methods are used. In offline path planning we can calculate full or almost full body dynamics that gives more accuracy for humanoid locomotion.

As it was already mentioned, in order to keep robot stable during locomotion we should generate such trajectory that keeps ZMP point inside of supporting polygon. Several techniques for generating walking motion for biped robots were proposed in the literature. For instance, in [11] polynomial trajectories were used, in [7] authors employed Fourier series. Katoh and Mori [12] demonstrated that using a Van der Pol oscillator as generator of the tracking reference would induce

walking trajectories for a biped robot. Furusho and Masubuchi [13] presented the walking control algorithms by tracking a piecewise-linear joint reference trajectory. Another method for trajectory generation is to mimic the human rhythmic function by means of a central pattern generator, just as it is reported in [14]. Kajita in [15] proposes ZMP tracking servo controller which adopts the preview control theory [16] that uses the future ZMP reference.

Gait parameter optimization is another important issue. It is important to decide optimal foot placements, CoM trajectory or walking speed considering constraints in joint actuators and energy efficiency. Goswami et al. applied genetic algorithm (GA) to maximize ZMP stability and step length by optimizing four gait parameters [17]. In addition, Dau et al. [18] planned foot and hip trajectories using polynomial interpolation and used GA to minimize the mechanical energy by optimizing the seven key parameters for the hip and foot trajectories. Liu et al. [19] designed ZMP trajectory to minimize an energy related function using fuzzy logic. In [20] authors applied dynamic programming approach to optimize walking primitives considering kinematic limits only.

Compared with previous works, our main problem was to estimate maximum walking speed, that can be achieved with given humanoid robot under actuator power and joint limit constraints. We used two approaches to solve the problem. The first, kinematic approach, operates only with robot kinematics and uses maximum joint velocities and accelerations. In dynamic approach we solved optimization problem with seven key walking parameters and with full body dynamics calculation.

The reminder of the paper is organized as follows. In Sect. 2 we formulate the problem. Section 3 focuses on kinematic approach in gait optimization. Section 4 presents dynamic approach for optimization problem. Finally, conclusions are drawn in Sect. 5.

2 Problem Statement

Majority of the algorithms for stable walking of a bipedal robot usually focus on balance control and do not take into account joint constraints. Therefore, calculated trajectories may be not reachable in practice because of velocity/acceleration/jerk limits in joints and lead to wrong foot positioning. On the other hand, there are works which study trajectory optimality with joints limits, but without stability analysis of such trajectories.

Anthropomorphic robot AR-601M [21] (Fig. 1), which is in the focus of our study, has 41 DoF in total, although during walking only 12 joints are used (6 in each pedipulator). For simplicity, we take into account that the robot motion lies in a sagittal plane. In this case, the problem of optimal trajectory can be reduced to the 5 DoF system.

The problem, which we analyse in our research can be formulated as following: find the optimal parameters of repeating steps motion such as step length, step time, hip height and etc., that maximize walking speed under robot constraints.

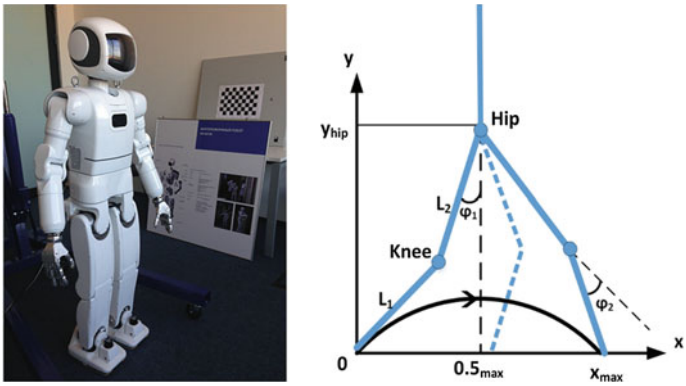

Fig. 1. Anthropomorphic robot AR-601M and its 5 DoF model in sagittal plane

3 Kinematic Approach

3.1 Dynamic Programming Method for Swing Leg Trajectory Optimization

In this approach the optimal trajectory problem does not consider trunk motion and can be is reduced to 2DoF system. Thus, the swing leg could be represented as a simple two-link system with hip and knee joints. The corresponding to AR601-M robot leg parameters link lengths are equal to 280 mm each. Since in our models robot body moves at a constant speed, for simplicity, its movement is ignored and we assume a fixed position of the hip joint. This means that considered problem is represented in a moving coordinate system. The trajectory of the swing leg and principle model parameters are shown in Fig. 1.

Optimization Criteria

There are different approaches to define cost function in optimal trajectory search problem. For example, Nakamura et.al. in [22] minimized energy consumption, which can be written in the form:

$$\sum_{i=1}^{2} \left[\tau_i \dot{\theta}_i + \gamma \tau_i^2 \right] dt \tag{1}$$

where τ_i is joint i torque, $\dot{\theta}_i$ is joint i velocity, γ is an empirical constant. The first term in (1) corresponds to mechanical work, which is performed to move dynamic system. The second term corresponds to heat emission in each joint due to torque generation. It was shown, that optimal trajectory which could be found in such a way well agrees with experimental data of human locomotion. Yet, while obtaining a swing leg trajectory, the authors do not take into account maximum joint velocity and acceleration limitations, which actually provide critical constraints for a real robot. A selected trajectory could be energy optimal

in theory, but if the robot's motors could not supply required by such trajectory torques, the physical robot will fail to perform such trajectory [23].

In practice, walking speed is one of the most important performance measures for bipedal robots. Walking speed could be unambiguously calculated, while energy consumption calculation is not that obvious as it depends on many factors; e.g., energy is mainly consumed in supporting leg joints, since they have much higher actuating torques than swing leg joints (in our work only swing leg motion is considered). In addition, energy consumption strongly correlates with step time: the faster a swing leg moves for a given step length, the lower is its energy consumption. Therefore, minimization of each step time is a critical issue to be considered, and it is the core contribution of our paper. Step time can be evaluated as

$$t = \int_S (1/V)\, dS \tag{2}$$

where V is a foot speed in Cartesian space and dS is the foot path. Time t is calculated numerically by dividing the trajectory into a finite number of intervals and further summing up over all intervals.

Search Algorithm.

Different techniques can be used to find swing leg optimal path of bipedal robot. For example, spline genetic algorithm (GA) in [22] determined a joint torque for several trajectory points and interpolated it for other points using third order spline. A significant drawback of this method is the GA algorithms feature of finding a global minimum for continues functions. A heuristic optimization method was used in [24] to find optimal trajectory with Harmony Search algorithm for 6 DoF manipulator. Smooth trajectories that comply kinematic constraints (velocity and acceleration) were obtained, but only 6 via-points between start and end points were used.

To overcome above mentions limitations, in this study, the optimal path is calculated using dynamic programming approach [25]. The key idea of this approach is to divide a large problem into sub-problems of lower dimensions corresponding to a transition between two via points, to solve each of these sub-problems once and to store the solutions. Advantages of this method are its robustness and computational efficiency compared to other methods. Illustration of this approach for simple case with two via points is shown in Fig. 2. To find an optimal path from node (1,1) to node (4,1) with a minimum total weight (time in our case) it is required to examine all possible connections between these points. Dynamic programing approach feature is that via points are not specified exactly and can be assigned to any node point of the row. Starting from the left, for every node minimal total weight W is computed and saved together with the node on the previous layer, transition from which is optimal. For example, for node (2,2) the minimal weight is 5 and the only transition from node (1,1) is possible. For node (3, 3) minimal weight is 10 (5+5), which corresponds to transition from node (2,2). Finally, we look at end point and find its optimal transition. After that, to get the optimal path, the optimal path from the last layer to the first

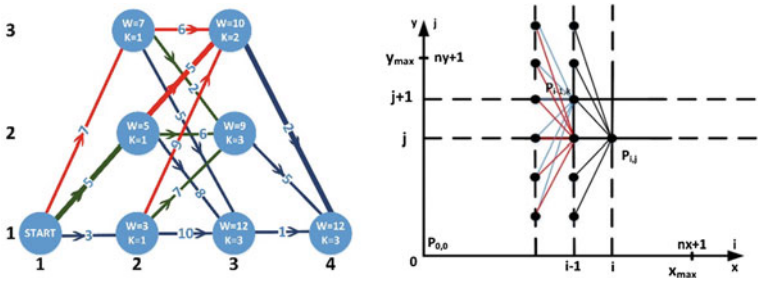

Fig. 2. Example of directed graph and building directed graph in search area by creating 2D grid

layer is constructed. For the provided example the optimal path corresponds to the following path: (4,1), (3,3), (2,2), (1,1).

To transform optimal path search problem for a bipedal robot into a directed graph it is required to put evenly distributed nodes $p_{i,j}$ within the search space, which covers all possible trajectory paths. Here it is required to create a two dimensional grid with n_x+1 points in x direction and n_y+1 points in y direction (see Fig. 2). Since we consider the trajectories with certain height limit $y_{\max}$ and step length $x_{\max}$ the desired search space size is equal to $x_{\max} \times y_{\max}$ area, which contains $n_x - 1$ via points to be assigned.

The algorithm for finding the optimal path works as follows:

- For each node point $p_{i,j},\ i = 1,\ j = \overline{1, ny+1}$ calculate the weight (i.e., the cost), which corresponds to the transition minimum time to that node from the start point $p_{0,0}$. In each node save the weight and joints angular velocities at the end of the corresponding trajectory.

- For each node $p_{i,j}$ where $i = \overline{2, nx},\ j = \overline{1, ny+1}$ calculate the weight of transition from $p_{i-1,\mathrm{k}}$ node, where $k = \overline{0, ny+1}$. Find $k_{\min}$, for which the sum of the calculated weight for transition from $p_{i,\mathrm{k}_{\min}}$ and total weight of $p_{i,\mathrm{k}_{\min}}$ node is minimal. In each node $p_{i,j}$ save $k_{\min}$, the total weight and joints angular velocities, which are calculated for the transition from $p_{i,\mathrm{k}_{\min}}$to $p_{i,j}$.

- For node $p_{\mathrm{nx}+1,0}$ (end point) calculate the weight of the transition from $p_{\mathrm{nx,k}}$, where $k = \overline{0, ny+1}$. Find $k_{\min}$, for which the sum of the calculated weight and the total weight of $p_{\mathrm{nx},\mathrm{k}_{\min}}$ node is minimal.

- Obtain an optimal trajectory by tracking backward $\mathrm{k}_{\min}$ values for each node:

$$p_{nx+1,ny+1} \rightarrow p_{nx,k_{\min}^{nx+1}} \rightarrow p_{nx-1,k_{\min}^{nx}} \rightarrow \ldots \rightarrow p_{1,k_{\min}^{2}} \rightarrow p_{0,0}$$

where $k_{\min}^{nx+1}$ is the optimal track for $p_{nx+1,ny+1}$node.

Since the transition time between two node points is used as a cost function, it is required to calculate minimal traveling time from node $p_{i-1,\mathrm{k}}$ to node $p_{i,j}$

taking into account velocity and acceleration limits. First of all, joint angles increments are calculated for each transition between two adjacent nodes. Then mark a joint as *active* if it has larger absolute value of angular increment for a given transition. Without loss of generality let's assume that joint 1 is active and joint 2 is passive. Assuming that active joint for each interval move either with a constant speed or a constant acceleration (depending whether it reaches the maximum velocity on previous interval), the joint movements can be described as follows

$$\Delta\varphi^{(i)} = \omega_s^{(i)} t + 0.5 a^{(i)} t^2 \tag{3}$$

$$\omega_e^{(i)} = \omega_s^{(i)} + a^{(i)} t \tag{4}$$

where i=1 for an active joint and i=2 for a passive joint, $\Delta\varphi$ is an angular increment,ω_s and ω_e are angular velocities at start and end of the interval respectively, a is an angular acceleration and t is a transition time.

In order to describe all possible relations between active joints on the adjacent intervals, three different cases for calculating transition time should be considered:

Case 1: Maximum Velocity. If an absolute angular velocity of an active joint in $p_{i-1,\mathrm{k}}$ node is equal to the maximum value $\omega_{\max}$ and its sign is equal to the sign of angular increment $\Delta\varphi$, then $t = \left|\Delta\varphi^{(1)}\right| / \omega_{\max}$, $a^{(1)} = 0$, $\omega_e^{(1)} = \omega_s^{(1)}$. Substituting t into equations (3) and (4) we obtain $a^{(2)}$, $\omega_e^{(2)}$. It should be emphasized that if the sign of angular increment $\Delta\varphi$ is opposite to the current velocity sign at the beginning of interval than either Case 2 or Case 3 should be considered.

Case 2: Maximum Acceleration. If an absolute angular velocity of an active joint in $p_{i-1,\mathrm{k}}$ node is below its maximum value $\omega_{\max}$ or its sign is opposite to the sign of angular increment $\Delta\varphi$, then we substitute $\Delta\varphi^{(1)}$ into equation (3) with $a^{(1)} = sign(\Delta\varphi^{(1)}) a_{\max}$ and solve the second order equation with respect to t:

$$t = \frac{-w_s^{(1)} \pm \sqrt{(w_s^{(1)})^2 + 2a^{(1)}\Delta\varphi^{(1)}}}{a^{(1)}}. \tag{5}$$

Next, we select the lower positive root of the above equation and calculate $\omega_e^{(1)} = \omega_s^{(1)} + a^{(1)} t$. If $\left|\omega_e^{(1)}\right|$ is less than or equal to $\omega_{\max}$, than $a^{(1)}$and $\omega_e^{(1)}$are equal to the calculated values. Finally, we substitute t into Eqs. (3)–(4) to obtain $a^{(2)}$, $\omega_e^{(2)}$.

Case 3: Reaching Maximum Velocity. If Case 1 condition is not satisfied and $\left|\omega_e^{(1)}\right|$in Case 2 is greater than $\omega_{\max}$, than $\omega_e^{(1)} = sign(\Delta\varphi^{(1)})\omega_{\max}$, $t = 2\Delta\varphi^{(1)}/(\omega_e^{(1)} + \omega_s^{(1)})$, $a^{(1)} = (\omega_e^{(1)} - \omega_s^{(1)})/t$. We substitute t into Eqs. (3)–(4) to obtain $a^{(2)}$, $\omega_e^{(2)}$. Figure 3 demonstrates all three cases which are described

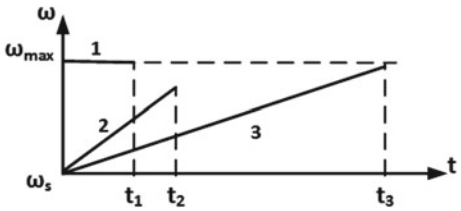

Fig. 3. Three cases of angular velocity behaviour: (*1*) maximum velocity; (*2*) maximum acceleration; (*3*) reaching maximum velocity

above. For all cases we verify if the calculated joint angular accelerations and velocities are below their maximal values. If this condition cannot be satisfied, this transition is excluded from a possible path of the swing leg.

Optimization Results.

The simulation of the algorithm was performed within MATLAB/Simulink environment. The acceleration and velocity limits were assigned to 1 rad/s^2 and 1 rad/s respectively for each joint. First, let us obtain optimal walking primitives for the fixed hip rising height and step length and then compare results with optimal parameters settings.

For the first case hip height was fixed to 0.5 m in order to ensure optimal locomotion speed of the robot based on our previous empirical studies [23,26]. According to joint limits and link parameters we selected the robot step length to be 0.4 m. For these parameters hip and knee joint angles in their starting position were set to 0.1 and 0.55 rad correspondingly; at the end of the trajectory (goal position) hip and knee joint angles were set to –0.66 and 0.55 rad correspondingly. These angles define $p_{i,j}$ and $p_{i,j}$ nodes.

Next, three different cases were analyzed:

(i) movement without any trajectory constraints, i.e. in an ideal case without velocity/acceleration limits the foot may move straightforwardly from a start point to an end point (Fig. 4 left);
(ii) movement with 0.1 m barrier (with negligible small size in the robot walking direction) in the middle of the trajectory (Fig. 4 right);
(iii) movement with 0.05 × 0.2 m box barrier in the middle (Fig. 5).

The results demonstrated that for all cases the obtained Cartesian trajectories of a swing leg do not correspond to the shortest path and differ from a cycloid path, which is traditionally used in bipedal robot locomotion control. To compare our results with a cycloid path approach, we built the cycloid trajectory for (ii) case and ensured the same travelling time as for our optimal trajectory (Fig. 4a right). The corresponding angular velocities are presented in Fig. 6. The simulation demonstrated that for the cycloid trajectory, the knee angular velocity exceeds maximum value and the accelerations at the beginning and at the end of the trajectory are very high. That means that in practice it is impossible

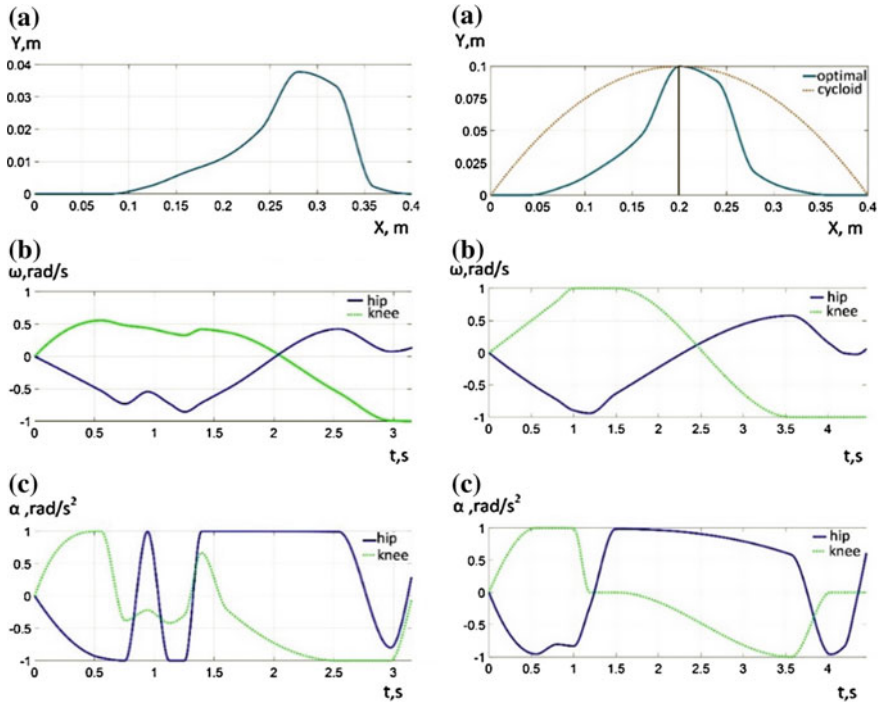

Fig. 4. Optimal trajectory without obstacles for hip height 0.5 m and step length 0.4 m (*left*) and trajectories with 0.1 m barrier in the *middle* for hip height 0.5 m and step length 0.4 m (*right*): **a** foot trajectory in Cartesian space; **b** angular velocity of joints; **c** angular acceleration of joints

to perform such trajectory within the specified time. In order to move along a cycloid trajectory, it is required to scale (increase) travelling time according to the velocity limits. Hence, the proposed algorithm succeeds to suggest a foot trajectory with a shorter time interval comparing to a typical cycloid trajectory.

In the case without trajectory constraints, the foot rises up to 0.04 m, which is caused by joint velocity/acceleration limits. It is evident that travel time in such case is minimum. The particularity of this trajectory is that the joint velocity limits are not reached (see Fig. 4b left).

Barrier profile essentially effects optimal trajectory (see Figs. 4a and 5a). Although the (ii) case barrier is two times lower than for case (iii), the height of the optimal trajectory for case (iii) and its travel time are higher.

To compare efficiency of the obtained walking primitives with conventional cycloids, the joint speed and acceleration profiles have been obtained for cycloids as well. It should be stressed, that these profiles do not satisfy velocity and acceleration limits, and to ensure such trajectory implementation it is required to increase traveling time. In particular, for free motions without obstacles the acceleration limits have been exceeded by the factor 6, and to remain within

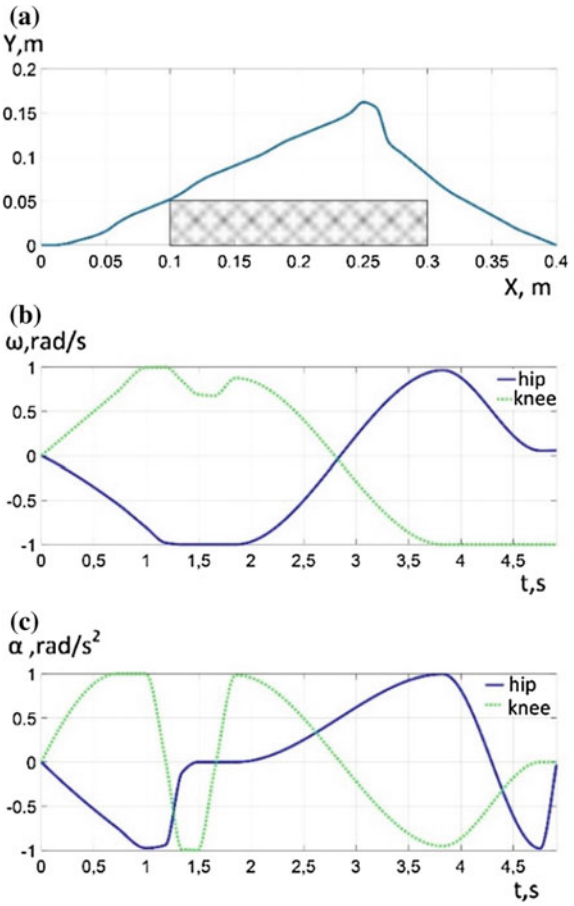

Fig. 5. Optimal trajectory with 0.05 × 0.2 m box barrier in the middle for hip height 0.5 m and step length 0.4 m: **a** optimal foot trajectory in Cartesian space; **b** angular velocity of joints; **c** angular acceleration of joints

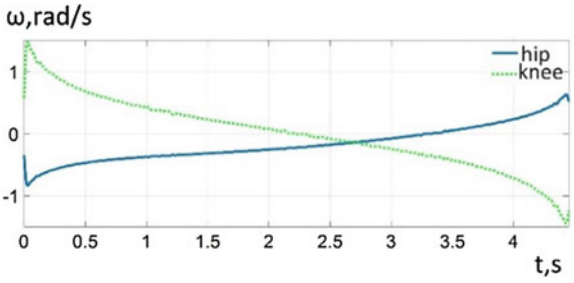

Fig. 6. Angular velocities of joints for cycloid trajectory movement with 0.1 m barrier, case of for hip height 0.5 m and step length 0.4 m

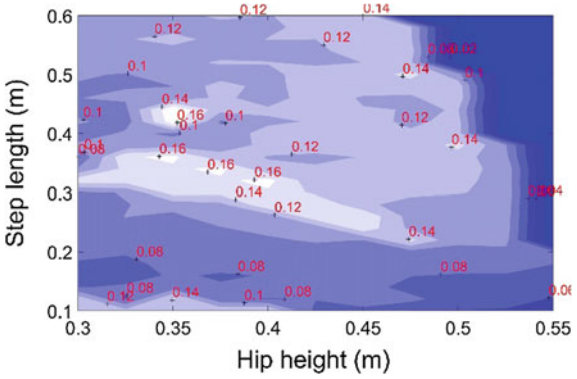

Fig. 7. Robot AR601M speed map for different step length and hip height for the trajectory without obstacles

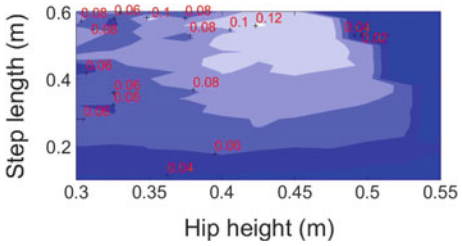

Fig. 8. Robot AR601M speed map for different step length and hip height for the trajectory with 0.1 m barrier in the middle

the limits traveling time should be over 10 s, which is twice higher that for the obtained optimal trajectory. Another limitation of conventional trajectory planning approach is its sensitivity to a swing height and request to provide traveling time as an input parameter. Our proposed approach does not have these limitations and automatically estimates minimal traveling time and an optimal swing leg height.

Now, let us obtain optimal hip heights and step length for all cases considered above and compare robot performance. Speed maps for different step length and hip height are presented in Figs. 7, 8 and 9. Here, lighter colour corresponds to higher speed and are preferable for robot locomotion. It is shown that Cartesian speed highly depends on the step length and hip height and varies from one case to another. It is also shown that optimal step parameters highly depend on the size of the obstacle, which appears on the robot path. In particular, for the case without obstacles optimal settings are hip height of 0.4 m and step length of 0.32 m, while for the case of box barrier the optimal step length is much higher (0.52 m) and hip height is almost the same (0.45 m).

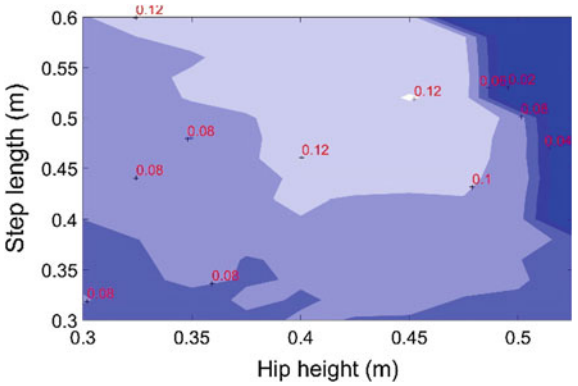

Fig. 9. Robot AR601M speed map for different step length and hip height for the trajectory with 0.05 × 0.2 m box barrier in the middle

Table 1. Optimal walking parameters for locomotion of bipedal humanoid robot AR-601M

Case	Step length (m)	Hip height (m)	Speed (m/s)	
			Fixed param.[a]	Optimal param.[b]
(i) without obstacles	0.32	0.40	0.13	0.16
(ii) with 0.1 m barrier	0.56	0.43	0.09	0.12
(iii) with 0.05 × 0.2 m box barrier	0.52	0.45	0.11	0.12

[a]Fixed hip and step length parameters are 0.5 and 0.4 m respectively
[b]Optimal hip height and step length parameters

Optimisation results are summarised in Table 1. Optimal walking parameters for locomotion of bipedal humanoid robot AR-601M, where for the three cases an optimal hip height, a step length and a corresponding robot speed are given. For comparison purposes it also contains robot speed for the case of a fixed hip height and step length studied above. It is shown that for the case of optimal hip and step size parameters robot speed increases by 10–23%, depending how far initial parameters were from the optimal ones.

For comparison purposes Fig. 10. Optimal trajectory without obstacles for 0.4 m hip height and 0.32 m step length: (a) foot trajectory in Cartesian space; (b) angular velocity of joints; (c) angular acceleration of joints contain walking primitives with joint velocities and accelerations for motion without obstacles.

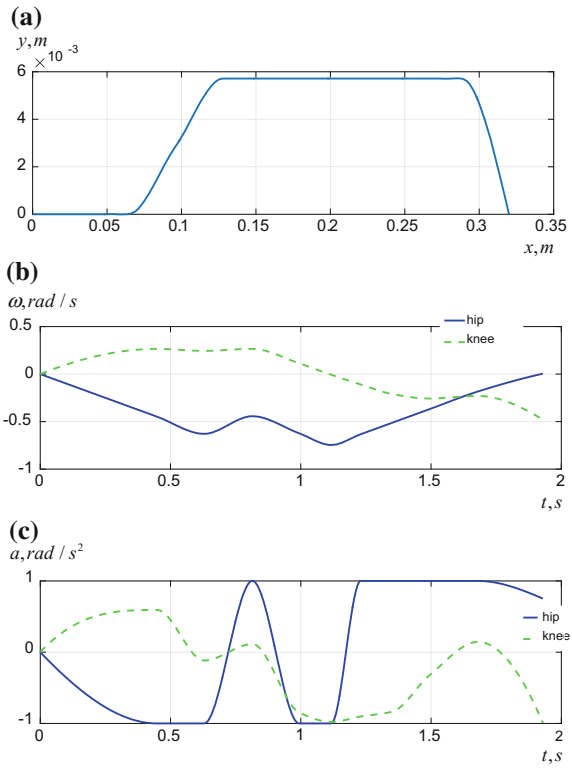

Fig. 10. Optimal trajectory without obstacles for 0.4 m hip height and 0.32 m step length: **a** foot trajectory in Cartesian space; **b** angular velocity of joints; **c** angular acceleration of joints

A rather evident fact that for an optimal robot speed without no obstacles, an optimal trajectory should be close to the ground level was confirmed by simulation results. It is clear that in practice such trajectory could be hardly implemented (in fact, it is not possible to have zero step height while locomotion), while it demonstrates efficiency of the proposed approach. With such moving primitive the robot can move with 0.16 m/s velocity instead of 0.13 that is maximal for 0.5 m hip height and 0.4 m step length. Similar tendencies are observed for all considered cases.

Advantages and Limitations.

In spite of numerous advantages, the proposed walking trajectory optimization approach has several apparent limitations, and the most significant one among them is ignoring of dynamic and static effects within optimization procedure. In fact, static effects (compliance errors) are not critical for the trajectory optimization since they are relatively small and could be easily compensated by integrating a feedback control from the feet force sensors. In this case the main limitation

for the moving primitive is avoiding joint coordinates limits, which may not allow the robot to compensate induced compliance errors. From another side, if feedback control is not available compliance errors should be computed using linear or non-linear stiffness modelling [27,28] and control algorithm should rely on the elasto-geometric model [29,30]. It should be stressed that stiffness parameters for real robot can be obtained from the dedicated experimental study only [31]. So, statics effects the control algorithm, but is not critical for optimization walking primitives.

On the other side dynamic effects directly influence robot stability [32,33] and can be hardly compensated, since this will directly affect walking primitive profile. Since walking profile contains only foot coordinate, humanoid torso and arms could be used to additionally increase robot balance [34,35]. From another side, integrating dynamic model into optimization procedure may provide additional tool for trajectory optimization. It may lead to faster robot movements in the case when joint acceleration will be induced not only because of actuation forces, but also by dynamic forces. However, this approach essentially complicates computations and may be hardly implemented for robot control through joint angles instead of demanded force level control. Besides, swing leg does not contribute a lot in robot dynamics since it does not effect robot body motion, which mostly defining robot stability. In contrast, it is a supporting that mainly defines CoM trajectory and, consequently, robot stability. From that point of view supporting leg trajectory could be unambiguously determined from stability condition while swing leg coordinates are redundant variables that might be optimised while step trajectory planning is proposed in this work. So, the suggested approach is a trade-off between a model complexity and utilization of robot total capacities. In practice, to avoid unpredictable robot behaviour, it is reasonable not to use upper velocity/acceleration boundaries in the optimization procedure since they may be higher in real model because of a presence of dynamic forces and errors in the model parameters.

The most essential limitation of the provided results is related to kinematic constraints induced to a hip location. It was strictly assumed that the hip height remains the same along the trajectory, while it is obvious that the best robot speed will be achieved when the height varies along the trajectory. In our approach, we separate swing and supporting leg movements and consider only a swing leg trajectory. Since a swing leg travels longer distances in walking, its joints should apply higher speeds and accelerations. Therefore, optimality due to kinematic limits is more important for a swing leg. We consider swing leg movement in coordinate system of a hip where the hip is fixed. Another direction for enhancing optimization efficiency is considering hip speed as an additional optimization parameter, which may vary from one via point to another. Providing reasonable solutions of the above-mentioned drawbacks and their integration into the optimization algorithm will apparently lead to robot speed increase. These issues will be addressed in details in our future work.

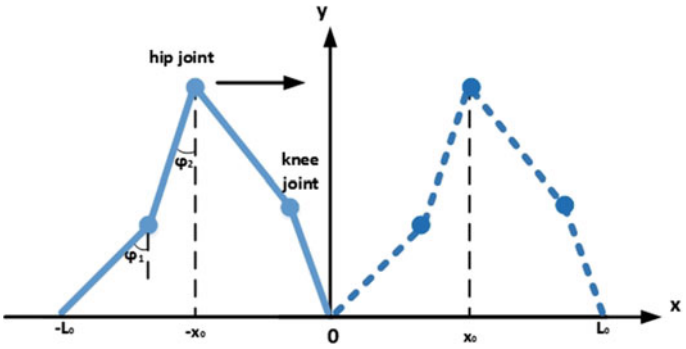

Fig. 11. Step motion of the swing and supporting legs in the sagittal plane

3.2 Trapezoidal Angular Velocity Profile Method

Method.

In this approach we consider one step motion with a symmetrical position at the start and end. The hip is located at the middle between two feet, i.e. $x_0 = L_0/2$. L_0 in our calculations is equal to 0.3 m, the hip height at start y_0 is equal to 0.5 (Fig. 11).

From manipulators theory we know that the actuators best performance is achieved when velocity profiles in joint space have trapezoidal form. In another words, the joint motion between two positions (in our case joint angles at start and end) should be done with maximum joint acceleration until maximum joint speed is reached and with maximum joint deceleration until end point.

Simulation Results.

In the simulation study, the acceleration and velocity limits were assigned to 1 rad/s2 and 1 rad/s for each joint. In addition, we calculated trajectories with maximum acceleration of 10 rad/s2.

Firstly, we calculated initial angles in joints using an inverse kinematics problem for a two link manipulator. Hip (q1) and knee (q2) angles are found according to following formulas:

$$q_2 = arccos\left(\frac{(x_{foot} - x_{hip})^2 + (y_{foot} - y_{hip})^2 - l_1^2 - l_2^2}{2l_1 l_2}\right) \tag{6}$$

$$q_1 = \text{atan2}\,(x_{foot} - x_{hip}, y_{foot} - y_{hip}) - \text{atan2}\,(l_2 \sin(q_2), l_1 + l_2 \cos(q_2)) \tag{7}$$

where l_1 and l_2 are upper and lower link lengths accordingly, x_{foot}, y_{foot}, x_{hip}, y_{hip} are foot and hip coordinates. For given initial and final parameters, hip and knee joint angles in the starting position are –0.08 and 0.74 rad, correspondingly, and at the end of the trajectory, they are –0.66 and 0.74 rad. As we see, the hip angle decreases, when knee angles are the same at the final position. Supposing that initial angular velocities are zero and that joint velocity profiles are symmetrically trapezoidal or triangular (the motion with maximum acceleration or

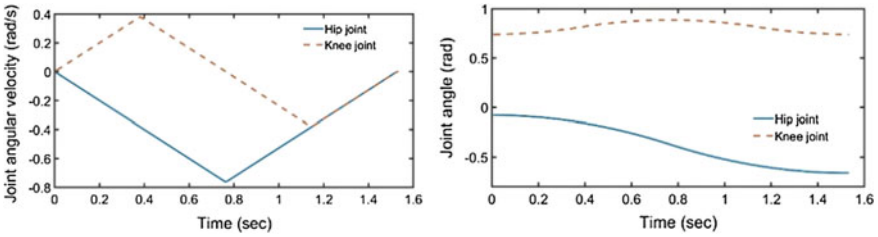

Fig. 12. Angular velocity profiles and joint angle profiles of the swing leg. A triangular case

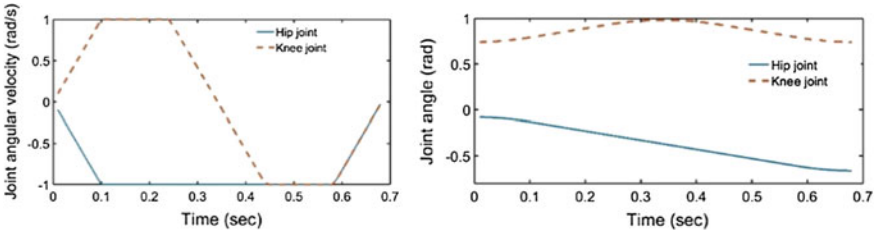

Fig. 13. Angular velocity profiles and joint angle profiles of the swing leg. A trapezoidal case

speed), we can find the time needed for hip joint angle change. After that, for the given time we define a velocity profile for the knee joint, again taking into consideration zero initial and final velocities, a symmetrical trapezoidal or triangular function with a total zero integral (angle change). Joint angle functions are found from velocity functions by integration with known initial values. Figures 12 and 13 show velocity and angle functions for acceleration limits 1 and 10 rad/s2 correspondingly. The motion time is 1.53 s for lower and 0.68 s for higher acceleration. We see that in the first case, the maximum velocities are not reached, when in the second case, profiles are trapezoidal. Since the motion is symmetrical, which means that final angles of the swing leg are initial angles of the supporting foot, we define velocity profiles of the supporting leg as profiles of the swing leg with an opposite sign.

After joint angle functions are found, we use the forward kinematics solution to find the foot trajectory in Cartesian space. Figure 14 shows foot trajectories for two acceleration limits. We see that in both cases, the foot is always above the ground, which is a necessary requirement.

However, the stability analysis of such trajectories shows that this kind of motion is unstable if there is no additional compensation of ZMP deviation from the stable one, corresponding to the center of the supporting foot. Therefore, such optimal trajectories are applicable only if we use the upper body motion to balance the robot dynamics during walking.

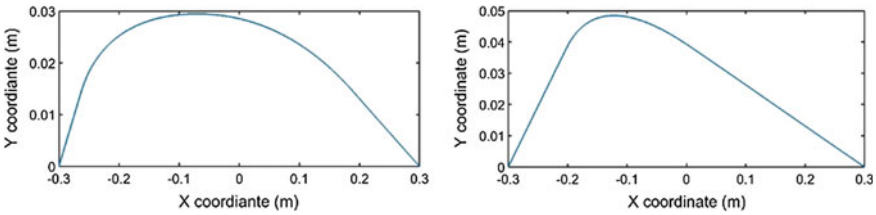

Fig. 14. The trajectory of the swing foot in Cartesian space for the lower (*left*) and higher (*right*) acceleration limit

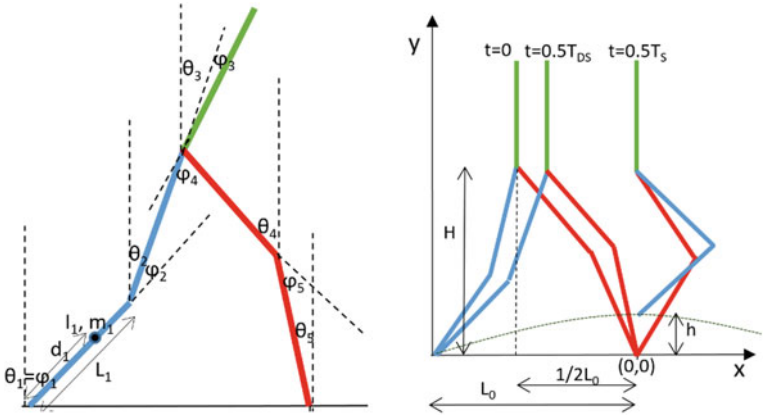

Fig. 15. Model of biped robot with 5 DoF and 5 links and Stick diagram of half walking cycle

4 Dynamic Approach

In dynamic approach the optimization problem is solved for 5 link model shown in Fig. 15. Model has 5 DoF and similar to kinematic approach considered above for 2D motion in sagittal plane. Length, mass and moment of inertia parameters of links are given in Table 2. These parameters correspond to the characteristics of AR601M.

Table 2. Manipulator link parameters

Link	L (m)	d (m)	Mass (kg)	Moment of inertia (kg*m^2)
Trunk	0.65	0.3	44.8	0.72
Thigh	0.28	0.14	6.8	0.055
Shank	0.28	0.12	3.9	0.038

Dynamic approach for searching optimal motion trajectory can be divided into following steps:

1. Parametrization of walking gait
2. Calculation of joint torques and velocities that ensure given trajectories
3. Stability investigation of walking pattern.

Search for the maximum motion speed under actuator and stability constraints.

4.1 Walking Gait Parametrization

Walking gait consists of two phases, Single Support and Double Support. If T_S is step time T_{SS} is single support phase time, T_{DS} is double support phase time than $T_S = T_{SS}+T_{DS}$, and ratio $DS = T_{DS}/T_S$. Figure 15 shows gait parameters. L_0 is step length, so swing foot moves from $-L_0$ to L_0 and due to symmetrical formulation of the problem hip moves from $-L_0/2$ to $L_0/2$. We assume that hip height during the step is fixed and is equal to H. Swing foot has symmetrical trajectory with its maximum height h. Trunk orientation is equal to zero. This means that it is always in vertical direction during walking.

Hip Trajectory.

In the dynamic approach hip trajectory in X direction is modeled with fifth order polynomial. All six parameters can be calculated given initial and final values for coordinate, velocity and acceleration.

Problem symmetry gives us equal velocity and acceleration in start and end points. If v_0 is initial velocity and a_0 is initial acceleration, then

$$\begin{aligned} &x_{hip} = c_5t^5 + c_4t^4 + c_3t^3 + c_2t^2 + c_1t + c_0 \\ &x_{hip}(0) = -L_0/2 \; x_{hip}(T_S) = L_0/2 \\ &v_{hip}(0) = v_{hip}(T_S) = v_0 \\ &a_{hip}(0) = a_{hip}(T_S) = a_0 \\ &y_{hip} = H \end{aligned} \tag{6}$$

Coefficients of polynomial are found from boundary conditions as following

$$\begin{aligned} &c_0 = -L_0/2 c_1 = V_0 \, c_2 = a_0/2 \\ &c_5 = \tfrac{(6d_2-3d_1)}{T_S^2} \\ &c_4 = \tfrac{\left(d_1-3d_2-2c_5T_S^2\right)}{T_S} \\ &c_3 = d_2 - c_5T_S^2 - c_4T_S \end{aligned} \tag{7}$$

where $d_1 = -\frac{2c_2}{T_S}$, $d_2 = \frac{L_0-c_1T_S-c_2T_S^2}{T_S^3}$

Swing Foot Trajectory.

In our work trigonometric functions are used to build trajectory profile, since they are simple and can provide zero velocities at contact moments. From the problem symmetry, we conclude that foot stays fixed for $0.5T_{DS}$ from beginning

and for $0.5\mathrm{T_{DS}}$ before the end, where $\mathrm{T_{DS}}$is double support time. Then foot trajectory is written as

$$\begin{aligned}
&x_{foot} = -L_0,\ if\ t < 0.5T_{DS}\\
&x_{foot} = -L_0\cos(\pi t/T_{SS}),\ if\ 0.5T_{DS} < t < T_S - 0.5T_{DS}\\
&x_{foot} = L_0,\ if\ t > T_S - 0.5T_{DS}\\
&y_{foot} = 0,\ if\ t < 0.5T_{DS}\\
&y_{foot} = 0.5h(1 - \cos(2\pi t/T_{SS})),\ if\ 0.5T_{DS} < t < T_S - 0.5T_{DS}\\
&y_{foot} = 0,\ if\ t > T_S - 0.5T_{DS}
\end{aligned} \tag{8}$$

4.2 Inverse Kinematics

Inverse kinematics problem solution is taken from kinematic approach. The only difference is related to angles notation (see Figs. 11 and 15.). Here, we define q_1^{sup} and q_2^{sup}as hip and knee joints of supporting foot and q_1^{SW} and q_2^{SW}as hip and knee joints of swing foot (see Fig. 11), then θ angles in Fig. 15 can be written as $\theta_1 = q_1^{\mathrm{sup}} + q_2^{\mathrm{sup}}$, $\theta_2 = q_1^{\mathrm{sup}}$, $\theta_4 = -q_1^{\mathrm{SW}}$, $\theta_5 = -q_1^{\mathrm{SW}} - q_2^{\mathrm{SW}}$. Angle θ_3 is independent from hip and foot positions and defined separately.

Besides joint angles we also need to find joint velocities and accelerations in each leg by using

$$\begin{aligned}
&\dot{q} = J(q)^{-1}\dot{X}\\
&\ddot{q} = J(q)^{-1}b\\
&b = \ddot{X} - \tfrac{d}{dt}(J(q)\dot{q})
\end{aligned} \tag{9}$$

where $J(q)$is Jacobian matrix, which can be computed from forward kinematics equations for each leg.

4.3 Inverse Dynamics

Inverse dynamics of the robot model is calculated for single support phase. Figure 15 shows robot parameters. Angles θ_i $(\mathrm{i} = 1, 2, 3, 4, 5)$ are sufficient to define the configuration. Firstly, we write Lagrange motion equation:

$$\frac{d}{dt}\left\{\frac{\partial K}{\partial \dot{q}_i}\right\} - \frac{\partial K}{\partial q_i} + \frac{\partial U}{\partial q_i} = Q_i\ (i = 1, 2\ldots, 5) \tag{10}$$

where K and U are the total kinetic and potential energy respectively, $q_i = \theta_i$. The equation can be converted to the following form:

$$D(\theta)\ddot{\theta} + h(\theta, \dot{\theta}) + G(\theta) = T_\theta \tag{11}$$

where $T_{\theta_i}$is generalized torque corresponding to θ_i angle. If we want to calculate driving torques, we should use the angles between links φ_i. The relationships between $\theta_i$and φ_i are the following:

$$\begin{aligned}
&\theta_1 = \varphi_1,\ \theta_2 = \varphi_1 - \varphi_2,\ \theta_3 = \varphi_1 - \varphi_2 - \varphi_3\\
&\theta_4 = -\varphi_1 + \varphi_2 + \varphi_3 + \varphi_4\\
&\theta_5 = -\varphi_1 + \varphi_2 + \varphi_3 + \varphi_4 - \varphi_5
\end{aligned} \tag{12}$$

Thus, from relation

$$T_{\varphi_i} = \sum_{j=1}^{5} T_{\theta_i} \frac{\partial_{\theta_j}}{\partial_{\varphi_i}},\ i = 1, \ldots, 5 \tag{13}$$

we can calculate driving torques.

4.4 Motion Stability

There are several stability criteria used in bipedal walking. Undoubtedly the most important stability criterion is based on the ZMP. The ZMP is the point on the ground where horizontal moments of ground-foot interaction are equal to zero.

The ZMP criterion says that the walking is stable if ZMP point is located inside support polygon. In our case ZMP coordinate can be calculated with the following formula:

$$x_{zmp} = \frac{\sum\limits_{i=1}^{5} m_i(\ddot{y}_i + g)x_i - \sum\limits_{i=1}^{5} m_i \ddot{x}_i y_i - \sum\limits_{i=1}^{5} J_i \ddot{q}_i}{\sum\limits_{i=1}^{5} m_i(\ddot{y}_i + g)} \tag{14}$$

where summation goes over each link with mass m_i, CoM coordinates $x_i y_i$, moment of inertia around CoM J_i and angular acceleration around CoM $\ddot{q}_i$.

4.5 Gait Optimization

The main goal of this optimization is to find the best motion gait pattern for the robot. Four parameters of the gait, initial hip accelerationa$_0$, initial velocity hip velocity v_0, step length L_0 and step period T_S are optimized in our work.

Method.

There are different gradient and non-gradient approaches that can be used to solve constrained optimization problem. In our work gradient based approach implemented in the Matlab (Mathworks, Inc.) function *fmincon* is used. To improve the robustness of the developed approach a number of initial points are used, which were randomly chosen within parameter bounds.

Objective Functions and Constraints.

Locomotion speed, which is calculated as $V = L_0/T_S$, was used as an objective function, which was maximized using *fmincon* function.

Actuator power and the ZMP criteria constraints were used in minimization problem. Actuator power was calculated as $P_i = |T_{\varphi_i}\dot{\varphi}_i|$. Its value should be less than P_{max} for each actuator. ZMP point during single support phase should lie closer to center of supporting foot. Since center of supporting foot has zero x coordinate, ZMP point coordinate, calculated by (14), should have absolute value less than zmp_{max}.

4.6 Optimization Results

Optimization problem was solved for five different double support time ratios: 15, 20, 25, 30, 35%; four different hip height: 0.4, 0.45, 0.5, 0.55 m; three different swing foot maximum height: 5, 10, 15 cm. Table 3, 4, 5, 6 and 7 present optimization results, optimal step length, optimal step time and maximum speed for each group of parameters.

Tables 8, 9 and 10 present maximum speed dependency on double support ratio, hip height and foot height. We see that maximum speed increases with DSR increase up to 25% and then decreases. It can be explained with the fact that initial increase of DSR improves robot stability and further increase shortens swing motion time and needs more power in actuators.

As expected, we see the best speed is shown when foot has the lowest trajectory, which means the lowest energy consumption. As for hip height, there is an optimal value of 0.45 m. Increase of height leads to shorter steps due to kine-

Table 3. Optimization results for double support ratio 15%

Hip height	Foot height		
	5 cm	10 cm	15 cm
0.4 m	0.58 m/s, 18 cm, 0.3 s	0.64 m/s, 26 cm, 0.40 s	0.58 m/s, 24 cm, 0.42 s
0.45 m	0.59 m/s, 18 cm, 0.3 s	0.58 m/s, 21 cm, 0.36 s	0.59 m/s, 23 cm, 0.39 s
0.5 m	0.57 m/s, 18 cm, 0.31 s	0.63 m/s, 31 cm, 0.49 s	0.51 m/s, 20 cm, 0.39 s
0.55 m	0.4 m/s, 14 cm, 0.34 s	0.28 m/s, 12 cm, 0.45 s	0.23 m/s, 13 cm, 0.57 s

Table 4. Optimization results for double support ratio 20%

Hip height	Foot height		
	5 cm	10 cm	15 cm
0.4 m	0.65 m/s, 27 cm, 0.42 s	0.59 m/s, 25 cm, 0.42 s	0.54 m/s, 24 cm, 0.44 s
0.45 m	0.64 m/s, 24 cm, 0.38 s	0.59 m/s, 24 cm, 0.41 s	0.61 m/s, 27 cm, 0.44 s
0.5 m	0.62 m/s, 24 cm, 0.39 s	0.57 m/s, 24 cm, 0.42 s	0.57 m/s, 26 cm, 0.45 s
0.55 m	0.37 m/s, 12 cm, 0.34 s	0.25 m/s, 12 cm, 0.5 s	0.2 m/s, 12 cm, 0.6 s

Table 5. Optimization results for double support ratio 25%

Hip height	Foot height		
	5 cm	10 cm	15 cm
0.4 m	0.64 m/s, 30 cm, 0.47 s	0.59 m/s, 29 cm, 0.50 s	0.55 m/s, 31 cm, 0.56 s
0.45 m	0.69 m/s, 34 cm, 0.50 s	0.64 m/s, 32 cm, 0.50 s	0.61 m/s, 31 cm, 0.51 s
0.5 m	0.65 m/s, 31 cm, 0.47 s	0.6 m/s, 29 cm, 0.48 s	0.53 m/s, 25 cm, 0.47 s
0.55 m	0.33 m/s, 11 cm, 0.34 s	0.23 m/s, 12 cm, 0.54 s	0.18 m/s, 12 cm, 0.64 s

Table 6. Optimization results for double support ratio 30%

Hip height	Foot height		
	5 cm	10 cm	15 cm
0.4 m	0.64 m/s, 35 cm, 0.56 s	0.59 m/s, 34 cm, 0.58 s	0.53 m/s, 34 cm, 0.65 s
0.45 m	0.67 m/s, 38 cm, 0.56 s	0.63 m/s, 36 cm, 0.57 s	0.58 m/s, 33 cm, 0.57 s
0.5 m	0.59 m/s, 29 cm, 0.49 s	0.55 m/s, 28 cm, 0.5 s	0.46 m/s, 24 cm, 0.52 s
0.55 m	0.3 m/s, 11 cm, 0.36 s	0.21 m/s, 11 cm, 0.54 s	0.17 m/s, 12 cm, 0.71 s

Table 7. Optimization results for double support ratio 35%

Hip height	Foot height		
	5 cm	10 cm	15 cm
0.4 m	0.62 m/s, 40 cm, 0.64 s	0.58 m/s, 40 cm, 0.69 s	0.51 m/s, 40 cm, 0.78 s
0.45 m	0.62 m/s, 37 cm, 0.6 s	0.59 m/s, 37 cm, 0.63 s	0.54 m/s, 33 cm, 0.61 s
0.5 m	0.57 m/s, 29 cm, 0.5 s	0.53 m/s, 27 cm, 0.5 s	0.42 m/s, 23 cm, 0.56 s
0.55 m	0.26 m/s, 10 cm, 0.4 s	0.18 m/s, 11 cm, 0.62 s	0.15 m/s, 11 cm, 0.73 s

matic constraints and we see sharp decrease in speed for 0.55 m height. Decrease of the height results in larger joint angle changes, therefore it is not optimal.

Table 8. Maximum speed for different double support ratio

	Double support phase				
	15%	20%	25%	30%	35%
Speed (m/s)	0.64	0.65	0.69	0.67	0.62

Table 9. Maximum speed for different hip height

	Y hip (m)			
	0.4	0.45	0.5	0.55
Speed (m/s)	0.65	0.69	0.65	0.4

Table 10. Maximum speed for different foot height

	Y hip (cm)		
	5	10	15
Speed (m/s)	0.69	0.64	0.65

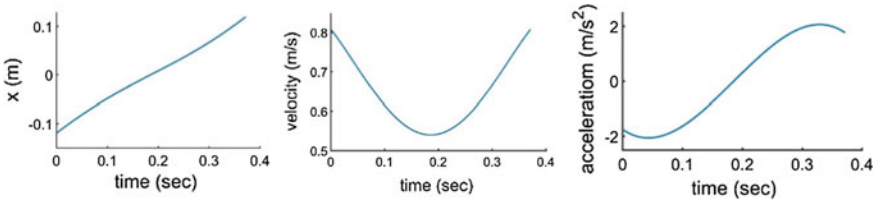

Fig. 16. Coordinate, velocity and acceleration of hip in x direction

Maximum speed of 0.69 m/s was obtained for 0.008 m/s^2 initial hip acceleration, 0.8715 m/s initial hip velocity, 0.34 m step length and 0.5 s step time for 25% double support ratio, 0.45 m hip height and 5 cm maximum foot height. Hip and joint trajectories and actuator power are shown in Figs. 16, 17 and 18.

It might be noted that knee joint of the swing leg has the highest angular velocity and acceleration. Here, joint acceleration exceeds 200 $1/s^2$, which is very high value at first glance. However, power values of the swing leg knee actuator are within the limit 300 Watt. Also, we can notice that power values of supporting ankle and swing hip joints are reached their maximum values (90 and 150 W). It means that these two actuators are subjected to critical loading.

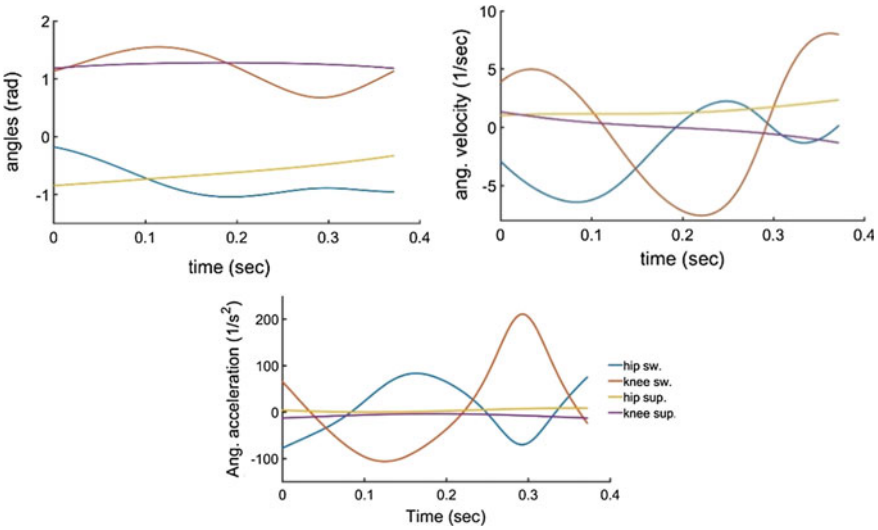

Fig. 17. Angles, angular velocity and angular acceleration of robot joints

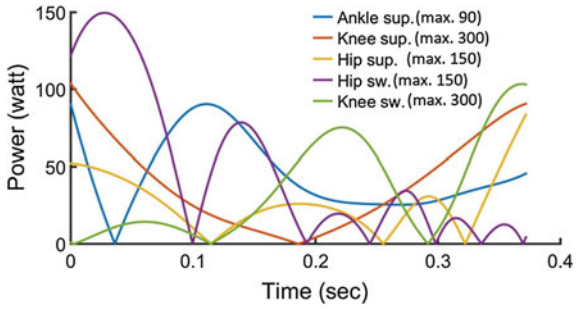

Fig. 18. Motor power in robot actuators

5 Conclusions

In the paper we considered a problem of optimization gait pattern for a bipedal robot, which maximizes its locomotion speed under joint angular velocity, acceleration and actuator power limits. We compared two approaches for defining the optimal leg trajectory of biped locomotion. The first one, kinematic approach, uses joint kinematic limits and utilizes dynamic programming and trapezoidal velocity profile methods to find trajectories where joints are rotated with possibly the maximum allowed speed or acceleration. However, the ZMP analysis of such trajectories shows that this kind of motion is unstable if there is no additional compensation of the ZMP deviation from the stable one, corresponding to the center of the supporting foot. Therefore, such optimal trajectories are

applicable only if we use the upper body motion to balance the robot dynamics during walking.

The second approach considers the robot dynamics and solves optimization problem to find maximum speed under actuator power and stability constraints. In contrast to kinematic approach, it allows us to use different velocity/acceleration limits depending on the payload applied to the actuated joint. This allowed us to reach physical limits for the swing leg. Simulation results show that robot can achieve speed up to 0.69 m/s.

Future research will be done in several directions. Firstly, the developed approach will be applied to frontal plane motion. Secondly, we will utilize vertical hip motion to increase our performance. And finally optimization problem will be solved not only for straight motion, but also for walking along arbitrary trajectories.

Acknowledgements. This research has been supported by Russian Ministry of Education and Science as a part of Scientific and Technological Research and Development Program of Russian Federation for 2014–2020 years (research grant ID RFMEFI60914X0004) and by Android Technics company, the industrial partner of the research.

References

1. Wright, J., Jordanov, I.: Intelligent approaches in locomotion - a review. J. Intell. Robot. Syst. **80**, 255–277 (2014)
2. Sakagami, Y., Watanabe, R., Aoyama, C., Matsunaga, S., Higaki, N., Fujimura, K.: The intelligent ASIMO: System Overview and Integration, pp. 2478–2483. IEEE, New York (2008)
3. Ogura, Y., Aikawa, H., Shimomura, K., Kondo, H., Morishima, A., Lim, H.-o., Takanishi, A.: Development of a New Humanoid Robot WABIAN-2. pp. 76-81. IEEE, New York (2006)
4. Shamsuddin, S., Ismail, L.I., Yussof, H., Zahari, N.I., Bahari, S., Hashim, H., Jaffar, A.: Humanoid Robot NAO: Review of Control and Motion Exploration. pp. 511–516. IEEE, New York (2011)
5. Feng, S., Whitman, E., Xinjilefu, X., Atkeson, C.G.: Optimization-based full body control for the DARPA robotics challenge. J. Field Robot. **32**, 293–312 (2015)
6. Vukobratovic, M., Borovac, B.: Zero-moment point - thirty five years of its life. Int. J. Hum. Robot. **01**, 157–173 (2004)
7. Shafii, N., Abdolmaleki, A., Lau, N., Reis, L.P.: Development of an Omnidirectional Walk Engine for Soccer Humanoid Robots (2015)
8. Albert, A., Gerth, W.: Analytic path planning algorithms for bipedal robots without a trunk. J. Intell. Robot. Syst. **36**, 109–127 (2003)
9. Sato, T., Sakaino, S., Ohnishi, K.: Real-time walking trajectory generation method with three-mass models at constant body height for three-dimensional biped robots. IEEE Trans. Indust. Electron. **58**, 376–383 (2011)
10. Ha, T., Choi, C.-H.: An effective trajectory generation method for bipedal walking. Robot. Autonom. Syst. **55**, 795–810 (2007)
11. Erik Cuevas, D.Z.: Polynomial Trajectory Algorithm for a Biped Robot (2010)

12. Katoh, R., Mori, M.: Control method of biped locomotion giving asymptotic stability of trajectory. Automatica **20**, 405–414 (1984)
13. Furusho, J., Masubuchi, M.: Control of a dynamical biped locomotion system for steady walking. J. Dyn. Syst. Meas. Control **108**, 111–118 (1986)
14. Liu, C., Wang, D., Chen, Q.: Central pattern generator inspired control for adaptive walking of biped robots. IEEE Trans. Syst. Man Cybern. Syst. **43**, 1206–1215 (2013)
15. Kajita, S., Kanehiro, F., Kaneko, K., Fujiwara, K., Harada, K., Yokoi, K., Hirukawa, H.: Biped walking pattern generation by using preview control of zero-moment point. In: Proceedings of the IEEE International Conference on Robotics and Automation, 2003. ICRA '03, vol. 1622, pp. 1620–1626 (2003)
16. Katayama, T., Ohki, T., Inoue, T., Kato, T.: Design of an optimal controller for a discrete-time system subject to previewable demand. Int. J. Control **41**, 677–699 (1985)
17. Goswami, A.: Postural stability of biped robots and the foot-rotation indicator (FRI) point. Int. J. Robot. Res. **18**, 523–533 (1999)
18. Dau, V.-H., Chew, C.-M., Poo, A.-N.: Achieving energy-efficient bipedal walking trajectory through GA-based optimization of key parameters. Int. J. Hum. Robot. **6**, 609–629 (2009)
19. Liu, Z., Wang, L., Chen, C.L.P., Zeng, X., Zhang, Y., Wang, Y.: Energy-efficiency-based gait control system architecture and algorithm for biped robots. IEEE Trans. Syst. Man. Cybern. Part C (Appl. Rev.) **42**, 926–933 (2012)
20. Khusainov, R., Klimchik, A., Magid, E.: Swing leg trajectory optimization for a humanoid robot locomotion. In: 2016 13th International Conference on Informatics in Control, Automation and Robotics (ICINCO) (2016)
21. Khusainov, R., Shimchik, I., Afanasyev, I., Magid, E.: Toward a human-like locomotion: modelling dynamically stable locomotion of an anthropomorphic robot in simulink environment. In: 2015 12th International Conference on Informatics in Control, Automation and Robotics (ICINCO), pp. 141–148 (2015)
22. Nakamura, M.: Trajectory planning for a leg swing during human walking. IEEE Int. Conf. Syst. Man Cybern. **1**, 784–790 (2004)
23. Khusainov, R., Sagitov, A., Afanasyev, I., Magid, E.: Bipedal robot locomotion modelling with virtual height inverted pendulum in Matlab-Simulink and ROS-Gazebo environments. J. Robot. Netw. Artif. Life **3** (2016)
24. Tangpattanakul, P., Artrit, P.: Minimum-time trajectory of robot manipulator using Harmony Search algorithm. In: 6th International Conference on Electrical Engineering/Electronics, Computer, Telecommunications and Information Technology, 2009. ECTI-CON 2009, pp. 354–357 (2009)
25. Si, J., Yang, L., Chao, L., Jian, S., Shengwei, M.: Approximate dynamic programming for continuous state and control problems. In: 17th Mediterranean Conference on Control and Automation, 2009. MED '09, pp. 1415–1420 (2012)
26. Khusainov, R., Afanasyev, I., Magid, E.: Anthropomorphic robot modelling with virtual height inverted pendulum approach in Simulink: step length and period influence on walking stability. In: The 2016 International Conference on Artificial Life and Robotics (ICAROB 2016), Japan (2016)
27. Klimchik, A., Pashkevich, A., Caro, S., Chablat, D.: Stiffness matrix of manipulators with passive joints: computational aspects. IEEE Trans. Robot. **28**, 955–958 (2012)
28. Klimchik, A., Chablat, D., Pashkevich, A.: Stiffness modeling for perfect and non-perfect parallel manipulators under internal and external loadings. Mech. Mach. Theory **79**, 1–28 (2014)

29. Klimchik, A., Pashkevich, A., Chablat, D., Hovland, G.: Compliance error compensation technique for parallel robots composed of non-perfect serial chains. Robot. Comput. Integr. Manufact. **29**, 385–393 (2013)
30. Klimchik, A., Bondarenko, D., Pashkevich, A., Briot, S., Furet, B.: Compliance Error Compensation in Robotic-Based Milling. In: Ferrier, J.-L., Bernard, A., Gusikhin, O., Madani, K. (eds.) Informatics in Control, Automation and Robotics: 9th International Conference, ICINCO 2012 Rome, Italy, July 28–31, 2012 Revised Selected Papers, pp. 197–216. Springer International Publishing, Cham (2014)
31. Klimchik, A., Furet, B., Caro, S., Pashkevich, A.: Identification of the manipulator stiffness model parameters in industrial environment. Mech. Mach. Theory **90**, 1–22 (2015)
32. Majima, K., Miyazaki, T., Ohishi, K.: Dynamic gait control of biped robot based on kinematics and motion description in Cartesian space. Electr. Eng. Jpn. **129**, 96–104 (1999)
33. Mitobe, K., Capi, G., Nasu, Y.: Control of walking robots based on manipulation of the zero moment point. Robotica **18**, 651–657 (2000)
34. Ude, A., Atkeson, C.G., Riley, M.: Programming full-body movements for humanoid robots by observation. Robot. Autonom. Syst. **47**, 93–108 (2004)
35. Yamaguchi, J., Soga, E., Inoue, S., Takanishi, A.: Development of a bipedal humanoid robot-control method of whole body cooperative dynamic biped walking. In: 1999 IEEE International Conference on Robotics and Automation, 1999. Proceedings, vol. 361, pp. 368–374 (1999)